Contents lists available at ScienceDirect

Science of the Total Environment

journal homepage: www.elsevier.com/locate/scitotenv

Functional relationships between aboveground and belowground spinach (*Spinacia oleracea* L., cv. Racoon) microbiomes impacted by salinity and drought

A. Mark Ibekwe [a,*], Selda Ors [b], Jorge F.S. Ferreira [a], Xuan Liu [a], Donald L. Suarez [a], Jincai Ma [c,d], Alaleh Ghasemimianaei [e], Ching-Hong Yang [e]

[a] US Salinity Laboratory, USDA-ARS, 450 W. Big Springs Rd., Riverside, CA 92507, USA
[b] Ataturk University, Department of Agricultural Structures and Irrigation, Erzurum 25240, Turkey
[c] Key Laboratory of Ground Water Resource and Environment, Ministry of Education, Jilin University, Changchun 130021, PR China
[d] College of New Energy and Environment, Jilin University, Changchun 130021, PR China
[e] Department of Biological Sciences, University of Wisconsin-Milwaukee, Milwaukee, WI 53211, USA

HIGHLIGHTS

- Proteobacteria, Bacteroidetes, and Actinobacteria accounted for most of the taxa detected.
- Monoterpenoid biosynthesis was the most significantly-enriched pathway in rhizosphere.
- The rhizosphere bacteria had the highest gene abundances.
- Salinity and drought affected the above- and belowground microbiomes differently.

GRAPHICAL ABSTRACT

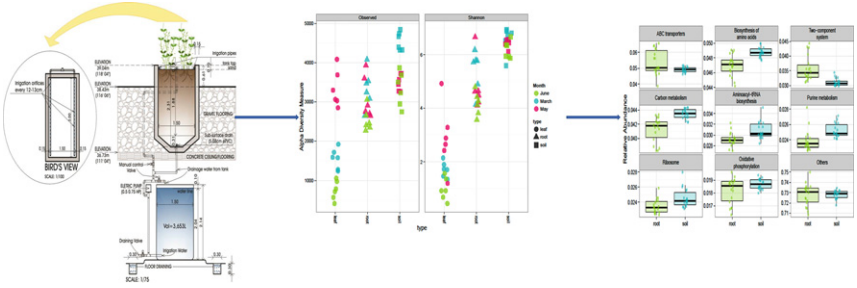

ARTICLE INFO

Article history:
Received 6 December 2019
Received in revised form 6 February 2020
Accepted 7 February 2020
Available online 08 February 2020

Editor: Damia Barcelo

Keywords:
Salinity
Seasonal changes
Piphillin
Soil microbial communities
Temporal variability
Inferred pathways
Genes

ABSTRACT

Salinity is a major problem facing agriculture in arid and semiarid regions of the world. This problem may vary among seasons affecting both above- and belowground plant microbiomes. However, very few studies have been conducted to examine the influence of salinity and drought on microbiomes and on their functional relationships. The objective for the study was to examine the effects of salinity and drought on above- and belowground spinach microbiomes and evaluate seasonal changes in their bacterial community composition and diversity. Furthermore, potential consequences for community functioning were assessed based on 16S V4 rRNA gene profiles by indirectly inferring the abundance of functional genes based on results obtained with Piphillin. The experiment was repeated three times from early fall to late spring in sand tanks planted with spinach (*Spinacia oleracea* L., cv. Racoon) grown with saline water of different concentrations and provided at different amounts. *Proteobacteria*, *Cyanobacteria*, and *Bacteroidetes* accounted for 77.1% of taxa detected in the rhizosphere; *Proteobacteria*, *Bacteroidetes*, and *Actinobacteria* accounted for 55.1% of taxa detected in soil, while *Proteobacteria*, *Firmicutes*, *Bacteroidetes*, and *Actinobacteria* accounted for 55.35% of taxa detected in the phyllosphere. Salinity significantly affected root microbiome beta-diversity according to weighted abundances ($p = 0.032$) but had no significant effect on the relative abundances of microbial taxa ($p = 0.568$). Pathways and functional genes analysis of soil, rhizosphere, and phyllosphere showed that the most abundant functional genes were mapped to membrane transport, DNA repair and recombination, signal transduction, purine

* Corresponding author at: USDA-ARS, U. S. Salinity Laboratory, 450 W. Big Springs Rd, Riverside, CA 92507, USA.
E-mail address: Mark.Ibekwe@ars.usda.gov (A.M. Ibekwe).

https://doi.org/10.1016/j.scitotenv.2020.137207
0048-9697/Published by Elsevier B.V.

metabolism, translation-related protein processing, oxidative phosphorylation, bacterial motility protein secretion, and membrane receptor proteins. Monoterpenoid biosynthesis was the most significantly enriched pathway in rhizosphere samples when compared to the soil samples. Overall, the predictive abundances indicate that, functionally, the rhizosphere bacteria had the highest gene abundances and that salinity and drought affected the above- and belowground microbiomes differently.

Published by Elsevier B.V.

1. Introduction

Soil water content may influence plant growth and persistence of microbes on the aboveground part of plants. This may be a function of water-use efficiency by plants due to salinity effects on soil water potential. Extended drought, caused by changes in weather patterns, can exacerbate the problem of salinity (Froelich et al., 2012). Salinity affects plants and microbes via two primary mechanisms: osmotic effect and specific ion toxicity (Oren, 1999; Chhabra, 1996). A change in soil salinity is frequently described as the single most important parameter determining the suitability of recycled water for agricultural irrigation (USEPA, 2004). The southwestern USA is expected to have increases in temperature, receive less springtime precipitation, and have more frequent and severe droughts during the next few years (Karl et al., 2009; Hellberg and Chu, 2015).

The analysis of metagenomic data from phyllosphere microbial communities has shown a correlation between taxonomic composition and community structure with environmental features (geography, climate, season, pollutant exposure, phytosanitary treatments), or even with the evolutionary history of the plant species or plant population (Bringel and Couée, 2015). These microorganisms must adjust to multiple fluctuations involving seasonal cycles, circadian cycles, and plant developmental stages. At the same time, plant water and other nutrients may not be readily available to leaf-surface microorganisms, thus making life extremely difficult for them to grow and multiply. Therefore, understanding of aboveground microbiota as providers of specific functions, for example, pathogen exclusion (Newton et al., 2010) and nitrogen fixation (Furnkranz et al., 2008) relies on continued efforts to catalog the microbial communities on plant foliage.

In this study, we investigated the implied functional responses of phyllosphere, soil and rhizosphere microbial community composition to increased salinity and drought, both associated with the climate of the southwestern United States. The paradigm of above- and belowground plant microbiomes controls most of the geochemical activities of plants. Recently, it was reported that microbial formation of stable carbon matter is more efficient from belowground than aboveground input (Sokol and Bradford, 2018). This increased stability is partly due to the greater efficiency of the microbial formation pathway by the rhizosphere microbial communities relative to bulk soil or the aboveground carbon sources (Sokol and Bradford, 2018). However, these authors suggested that the bulk soil had greater capacity to form mineral-stabilized soil carbon due to its greater overall volume, and that the relative contributions of aboveground versus belowground carbon inputs depended greatly on the ratio of rhizosphere to bulk soil.

Microbiome community and changes thereof due to environmental parameters generally are described using 16S rRNA gene sequencing methods, while mechanistic information on these changes require functional analysis (Koo et al., 2017). Shotgun sequencing is the most effective method of analyzing the functional capabilities of microbial communities by allowing detection and quantification of functional genes. However, in recent years, new metagenomics inference tool that utilizes 16S rRNA data to predict the functional attributes of microbial assemblages have been introduced. These include PICRUSt (Langille et al., 2013), Tax4Fun (Aßhauer et al., 2015), and Piphillin (Iwai et al., 2016). These metagenomics inference tools derive functional gene content of microorganisms based on the known genome information of bacteria closest to their taxonomic lineage (Koo et al., 2017). The 16S rRNA data from these metagenomics inference tool and the Kyoto Encyclopedia of Genes and Genomes (KEGG) database are compared to predict functional attributes of microbial communities in the studied environment. It is now well established that reciprocal interactions between aboveground and belowground communities not only shape the structure and functioning of terrestrial ecosystems but also, they regulate their response to global change across a hierarchy of temporal and spatial scales (Bardgett, 2018; Jansson and Hofmockel, 2018).

The study investigated the above and belowground microbial community compositions and their inferred functions in response to seasonal climate trends associated with different soil salinity levels and drought in an outdoor lysimeter experiment. The main hypothesis for the study was that bacterial community composition across the experimental plots (lysimeter) would change across different growing seasons. The main objectives of the study were to determine bacterial community richness and composition in response to seasonal changes under different soil salinities and to determine which groups of bacterial responds differently due to changes in season. Three experiments were conducted during winter, spring, and summer to coincide with spinach growing season in the southwestern United States. Most of the summer spinach production is done from April to October in California's Salinas Valley, while winter production (from November to March) takes place in the desert regions of Yuma, Arizona and California's Imperial Valley.

2. Materials and methods

2.1. Field setup and experimental treatments

The study was carried out in lysimeters (sand tanks) containing loamy sand mixed with 10% peat moss (on a volume basis) with an average bulk density of 1.38 g/cm^3, and with an average volumetric water content of 0.30 m^3/m^3 at saturation (Ors and Suarez, 2017; Ibekwe et al., 2017). Geochemical characteristics of the soil and chemical composition of the salinity treatments used for the study had previously been published (Ors and Suarez, 2016). The sand tanks consisted of 24 units planted with spinach and used to determine the interactive effects of salinity and drought treatments on above- and belowground microbiomes of spinach (*Spinacia oleracea* L., cv. Racoon). The first and second sets of experiments started on 7 December 2012 and 14 March 2013, respectively, in large sand tanks (3.0 m L × 1.5 m W × 2.0 m D), while the third experiment started on 9 April 2013 in small sand tanks (202.5 cm L × 81.5 cm W × 85 cm D). Seeds were planted in three rows 40 cm between rows in sand tanks at 10 cm apart and thinned to 25 plants per row.

Measurements of the water content (θ) of the substrate were accomplished using calibrated ($\ln(\theta) = -6.99 + 16\,V - 9.9\,V2$, $R^2 = 0.91$) dielectric soil moisture sensors (ECH_2O-10 probes, Decagon, Pullman, WA, USA1) inserted at 10 cm depth. A total of 16 ECH2O moisture sensors were used in the study. The ECH_2O moisture sensors were connected to a multiplexer (AM25T, Campbell Sci., Logan, UT, USA), which in turn was connected to a data logger (CR10X, Campbell Sci.) to record the sensor output. The water retention curve was determined using the pressure plate method (Klute, 1986). The measured water contents from the sensors were then converted to matric potential using the water retention curve. Drought treatments were designed with soil water matric pressure targets of D1 (−200 to −300 kPa), treatment D2 (−400 to −500 kPa) and control D0 (no water stress, >−45 kPa).

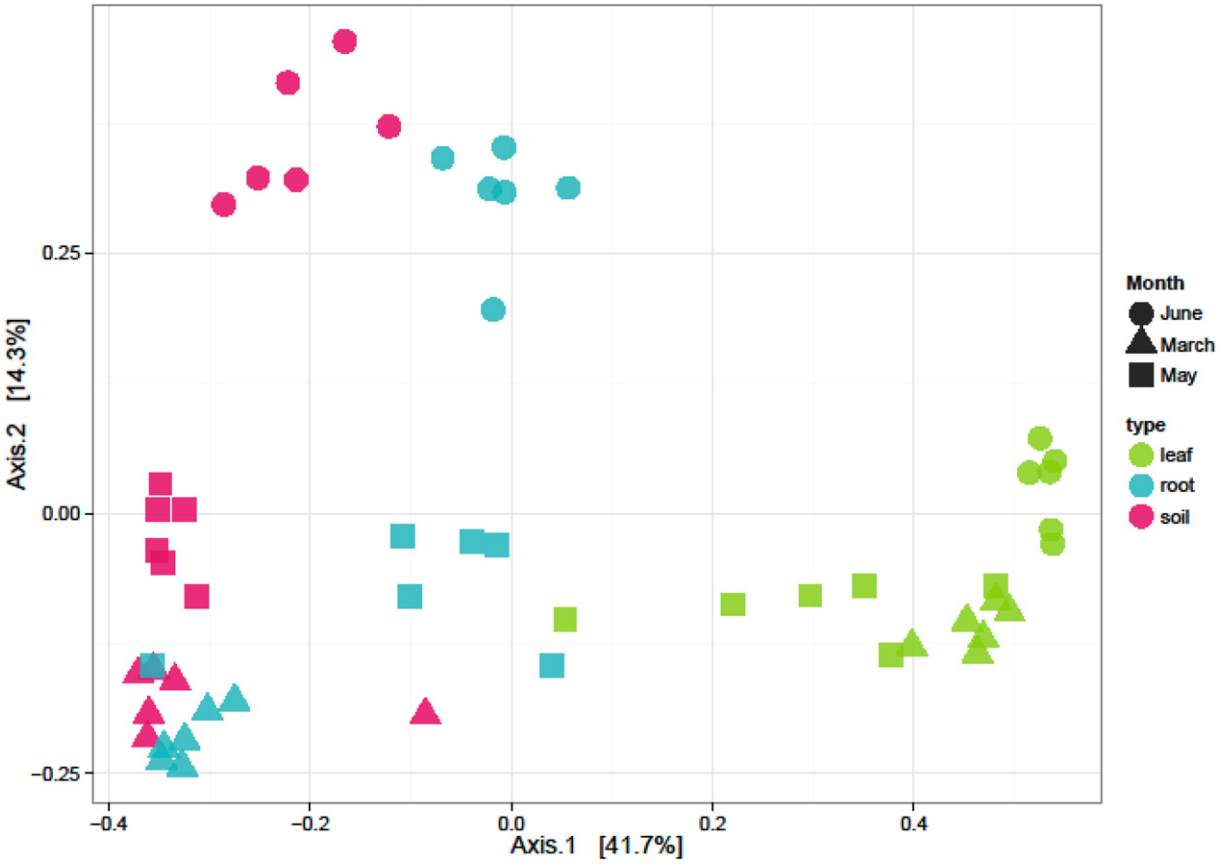

Fig. 1. Dimensional reduction of the Bray-Curtis distance between microbiome samples, using the PCoA ordination method.

Higher irrigation frequencies were maintained in control D0 than in drought D1 and D2, in accordance with instrument readings to keep matric potential within the specified limits (in kPa) (Ors and Suarez, 2017). Each sand tank was irrigated with solutions prepared in an individual reservoir (1.5 m diameter×2.2 m deep). Irrigation water with 1) modified half-strength Hoagland's nutrient solution and 2) with salt solutions were pumped from water reservoirs (vol. = 3605 L for large sand tanks) housed underneath the tank facility to the sand tanks above, completely saturating and leaching the sand culture medium. For each tank the nutrient/salt solution returned to the reservoir after each irrigation cycle, through a subsurface drainage system at the bottom of the tanks, thus maintaining an essentially uniform and constant salinity in the root zone (Ors and Suarez, 2016). The third experiment was conducted in smaller sand tanks (Poss et al., 2004) consisting of 24 experimental plant growth units containing loamy sand with an average bulk density of 1.4 g cm^{-3} with planting on the date shown above and irrigated from individual reservoirs (1740-L) containing a modified half-strength Hoagland's nutrient solution combined with various concentrations of NaCl and other salts to achieve target salinities, measured as electrical conductivity (EC_{iw}) and expressed in dS m^{-1}. The system was initially flushed with a nutrient solution made up in Riverside tap water (EC_{iw} = 0.65 dS m^{-1}) so also was the source water for irrigation.

Nutrient solution used for the study was modified half Hoagland's solution added of (in $mmoles_c$ L^{-1}): 2.5 Ca $(NO_3)_2$, 3.0 KNO_3, 0.17 KH_2PO_4, 1.5 $MgSO_4$, 0.05 Fe as sodium ferric diethylenetriamine pentaacetate (NaFe-EDTA), 0.023 H_3BO_3, 0.005 $MnSO_4$, 0.0004 $ZnSO_4$, 0.0002 $CuSO_4$, and 0.0001 H_3MoO_4. Low-salinity control (EC_{iw} = 0.85 dS m^{-1}) was the base nutrient solution without added salts in all experiments. Electrical conductivities of the irrigation waters (EC_{iw}) were 4, 7, 9, 12, and 15 dS m^{-1}, achieved by adding $CaCl_2$, $MgCl_2$, NaCl, Na_2SO_4 to the base tap water-nutrient solution (low-salinity control). Salt concentrations used were as previously described and based on EXTRACT Chem model (Suarez and Taber, 2012) to predict the ion composition needed to achieve the target EC_{iw} values. After the first pair of true leaves was fully expanded on all the plants, salinity treatments were initiated, and salt was added to the irrigation water in four equal increments over a four-day period to avoid osmotic shock to the seedlings. Sand tanks were irrigated once daily for large tanks and twice for small tanks to completely saturate the culture medium in non-drought treatments. The first experiment was a complete randomized design with three replications and four salinity treatments including control (EC_{iw} = 0.85 dS m^{-1}) and two different saline water types, dominated by either sulfate or by chloride ions. The second and third experiments had 6 different salinity levels including control treatment (EC_{iw} < 0.85 dS m^{-1}) and only chloride-dominated water type. In subsequent experiments we used only chloride-dominated water type as the first experiment did not show any statistical differences in spinach yields, at any salinity levels, between sulfate- and chloride-dominated water types.

Chemical composition of the salinity water treatments used in the experiments was reported elsewhere (Ors and Suarez, 2016). The concentrations of Na, K, Mg, Ca, and total- S on plant samples were determined from nitric acid digestions by inductively coupled plasma optical emission spectrometry (ICP-OES). The average temperatures (°C) and reference evapotranspiration (ET_0) that occurred during the experiment was acquired from the California Irrigation Management Systems (CIMIS) weather station no. 44 at the University of California Riverside, California (Koike et al., 2011), and the temperature trend for weather station no. 44 during the past 20 years was recently reported (Ibekwe et al., 2017).

2.2. DNA extraction and V4 16S sequencing

DNA was extracted from plant samples for microbiome analysis collected from triplicate plots at the end of the experiment. Ten grams of

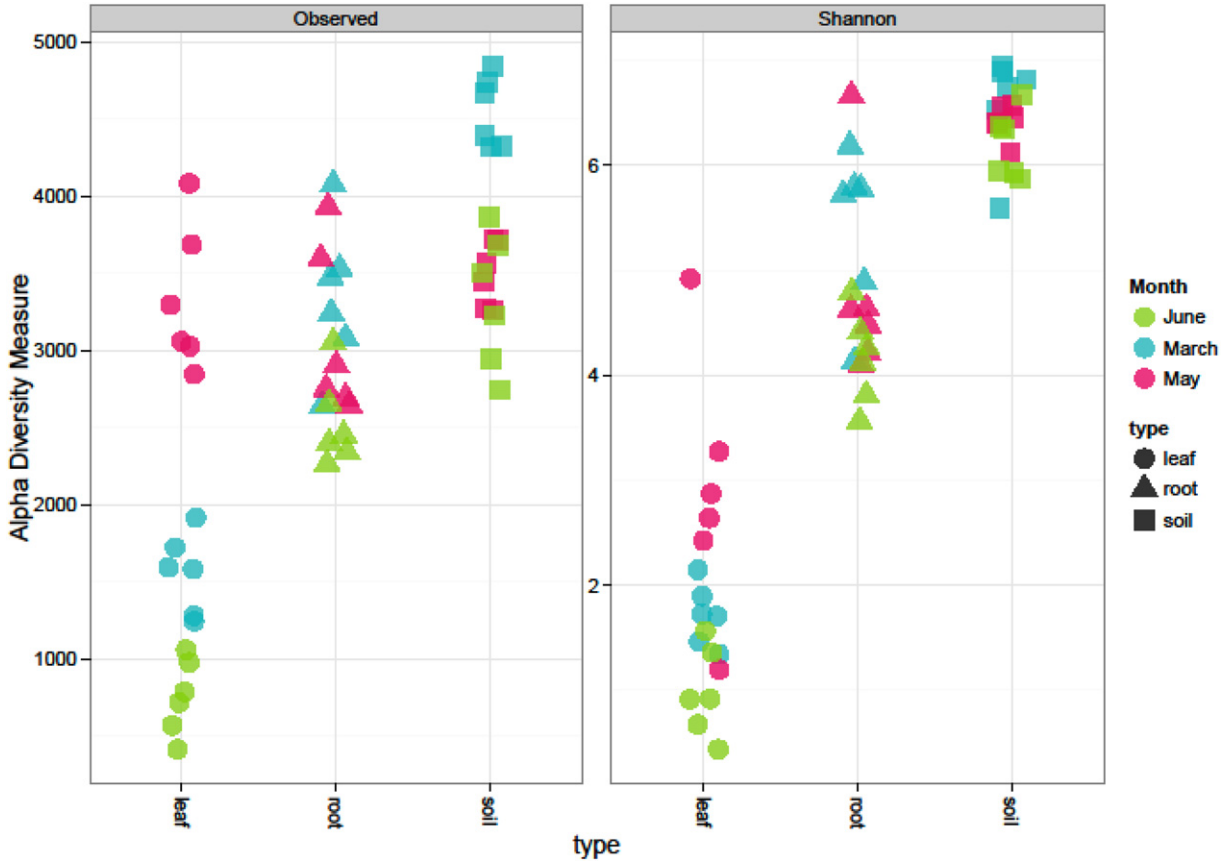

Fig. 2. Alpha-diversity estimates. Soil samples had higher alpha diversity than root or leaf samples.

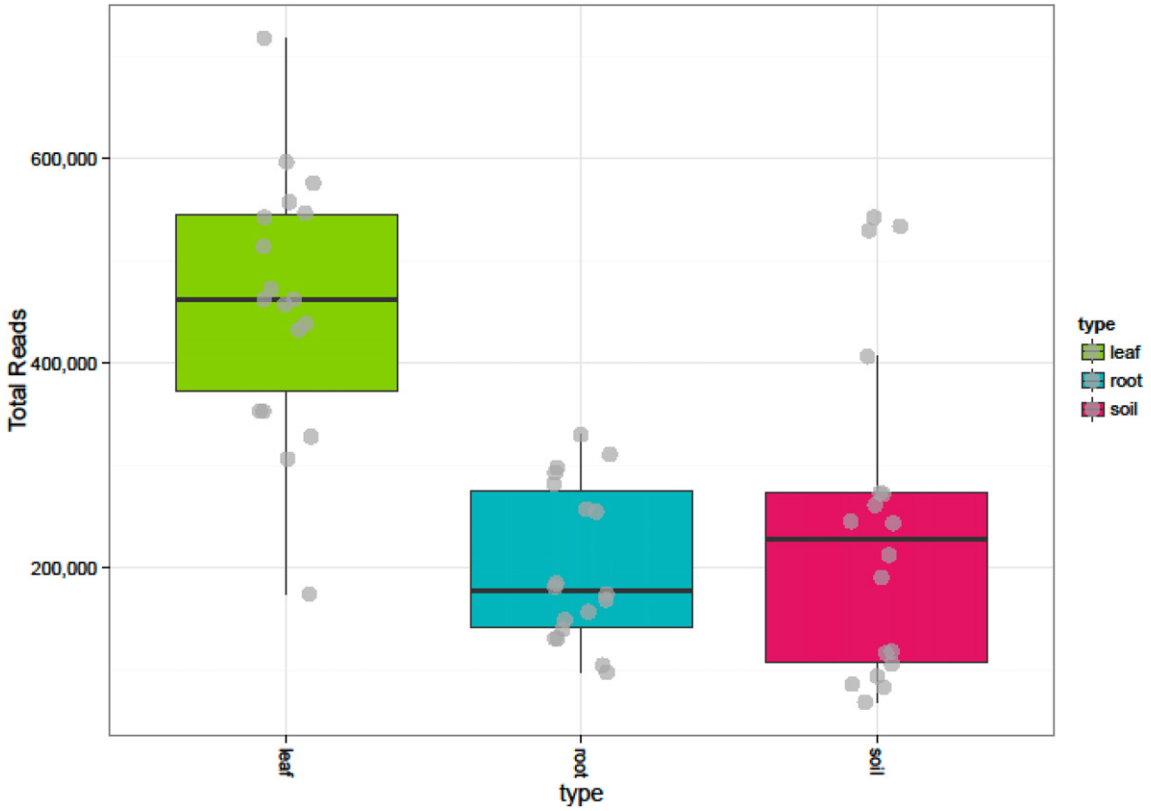

Fig. 3. Sample library size. Each point above represents the number of reads in a sample. Sequences per sample ranged from a minimum of 68,440 to a maximum of 717,922 filtered reads.

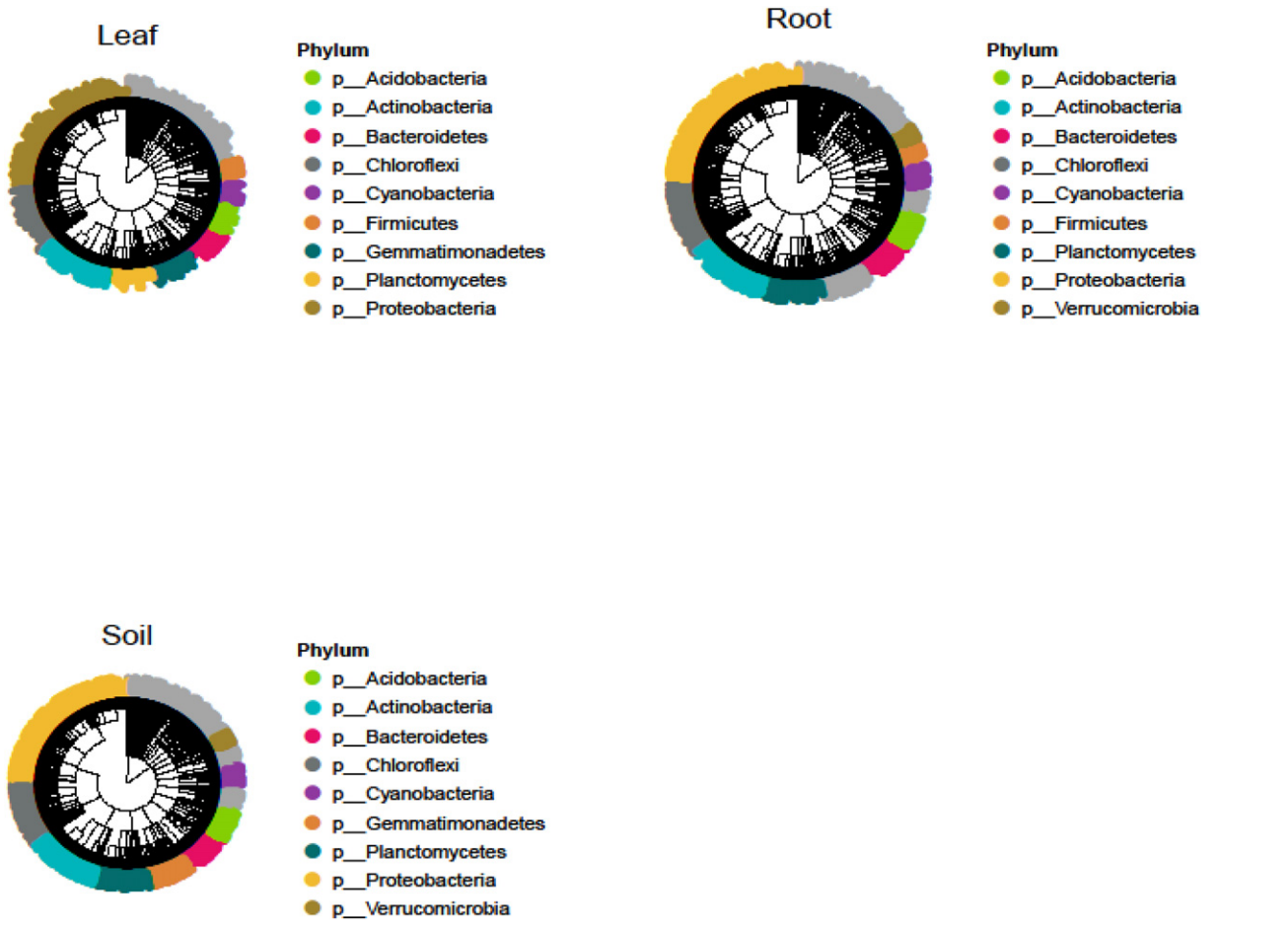

Fig. 4. Phylogenetic tree at the phylum rank. The height of each bar indicates the number of samples containing that phylum. The most abundant -level clades are colored with the remainders in light gray. (For interpretation of the references to color in this figure legend, the reader is referred to the web version of this article.)

non-rhizosphere soil samples were collected at least 10 cm away from plants, and rhizosphere samples were collected after shaking loosely-held soil from roots into stomacher bags and weighed. At the same time, leaf samples were cut above the soil surface with a sterile blade placed in the stomacher bags and weighed. Community DNA was extracted from the three sample types with the Power Soil DNA Kit (MoBio Laboratories, Solana Beach, CA) and stored at −20 °C after further cleanup steps with DNA Clean and Concentrator (Zymo Research Corp- Irvine CA). The cleaned-up samples were used for MiSeq sequencing after quantification with a Nanodrop ND-2000 C spectrophotometer (Nanodrop Technologies, Wilmington DE), run on 1.0% agarose gel and passed through additional cleanup before sequencing. DNA samples were profiled using Second Genome's Microbiome Signature Discovery service (San Bruno, CA, USA), Illumina sequencing assays to track microbial population dynamics above and below plants, KEGG Pathways, and genes profiles across the three planting seasons.

2.3. Profiling method and library preparation

To enrich the sample for bacterial 16S V4 rDNA region, DNA was amplified utilizing fusion primers designed against the surrounding conserved regions which are tailed with sequences to incorporate Illumina (San Diego, CA) adapters and indexing barcodes. Each sample was PCR amplified with two different bar coded V4 fusion primers 515F (5′-GTGCCAGCMGCCGCGGTAA-3′) and 806R (5′-GGAC TACVSGGGTATCTAAT-3′) (Caporaso et al., 2011), and PCR products were quantified by fluorometric method (Qubit or PicoGreen from Invitrogen, Life Technologies, Grand Island, NY). Samples that met the post-PCR quantification minimum were pooled equimolar and advanced for sequencing. A pool containing 16S V4 enriched, amplified, bar-coded samples were loaded into a MiSeq® reagent cartridge, and then onto the instrument along with the flow cell. After cluster formation on the MiSeq instrument, the amplicons were sequenced for 250 cycles with custom primers designed for paired-end sequencing.

2.4. Data analysis methods

Representative OTU sequences were assigned taxonomic classification via Mothur's Bayesian classifier, trained against the Greengenes reference database of 16S rRNA gene sequences and clustered at 99% (McDonald et al., 2012). Sequenced paired-end reads were merged using USEARCH and the resulting sequences were compared to an in-house strain database using USEARCH (Edgar, 2010). All sequences hitting a unique strain with identity ≥99% were assigned a strain Operation Taxonomic Unit (OTU). To ensure specificity of the strain hits, a difference of ≥0.25% between the identity of the best hit and the second-best hit was required (e.g. 99.75 versus 99.5). For each strain OTU, one of the matching reads was selected as representative and all sequences were mapped by USEARCH against the strain OTU representatives to calculate strain abundances. The remaining non-strain sequences were quality- filtered and dereplicated with USEARCH (Edgar, 2010). Resulting unique sequences were then clustered at 97% by UPARSE (de novo OTU clustering) and a representative consensus sequence per de novo OTU was determined (Edgar, 2013). The UPARSE clustering algorithm comprises a chimera filtering feature that discards likely chimeric OTUs. All non-strain sequences that passed the quality filtering

were mapped to the representative consensus sequences to generate an abundance table for de novo OTUs. After the taxa were identified for inclusion in the analysis, the values used for each taxa-sample intersection were populated with the abundance of reads assigned to each OTU in an 'OTU table'. A corresponding table of OTU Greengenes classification was generated as well. Alpha-diversity (within sample diversity) metrics were calculated to estimate sample richness and Shannon diversity. Beta-diversity (sample-to-sample dissimilarity) metrics were calculated for the inter-comparison in a pair-wise fashion to determine dissimilarity score and stored in a distance dissimilarity matrix. Abundance-weighted sample pair-wise differences were calculated using the Bray-Curtis dissimilarity. All analyses were generated using Second Genome R package (vegan: R package version 2.2-1). Bray-Curtis dissimilarity was calculated by the ratio of the summed absolute differences in counts to the sum of abundances in the two samples using the Jaccard index. Hierarchical clustering maps of the samples in the form of dendrograms and principal coordinate analysis (PCoA) were used to visualize complex relationships between samples. Permutational analysis of variance (PERMANOVA) was utilized to find significant differences among discrete categorical or continuous variables based on the Monte Carlo permutation test. Univariate differential abundance of OTUs was tested using negative binomial noise model for the overdispersion and Poisson process intrinsic to this data, as implemented in the DESeq2 package (Love et al., 2014) and described for microbiome applications in (McMurdie and Holmes, 2013).

2.5. Inference of metagenomes

Piphillin was developed to leverage the most up-to-date genome database for metagenome prediction from 16S rRNA sequence data (Iwai et al., 2016), using the KEGG 70.1 (Kyoto Encyclopedia of Genes and Genomes) orthologues database. A genome was inferred for each 16S rRNA OTU based on the sequence identity between an OTU's representative sequence and the nearest neighbor 16S rRNA sequence from the genome databases restricted to a minimum identity of 97%. Then, OTU abundance was normalized by 16S rRNA copy numbers and further multiplied by the gene contents of each inferred genome to predict each sample's metagenome. To identify differentially abundant KEGG pathways and genes, a Wilcoxon Rank Sum test was employed. Where samples could be paired across categories, a paired Wilcoxon signed rank test was used. *P*-values were adjusted by the Benjamini-Hochberg procedure to weed out false discovery rates from multiple testing (Benjamini and Hochberg, 1995).

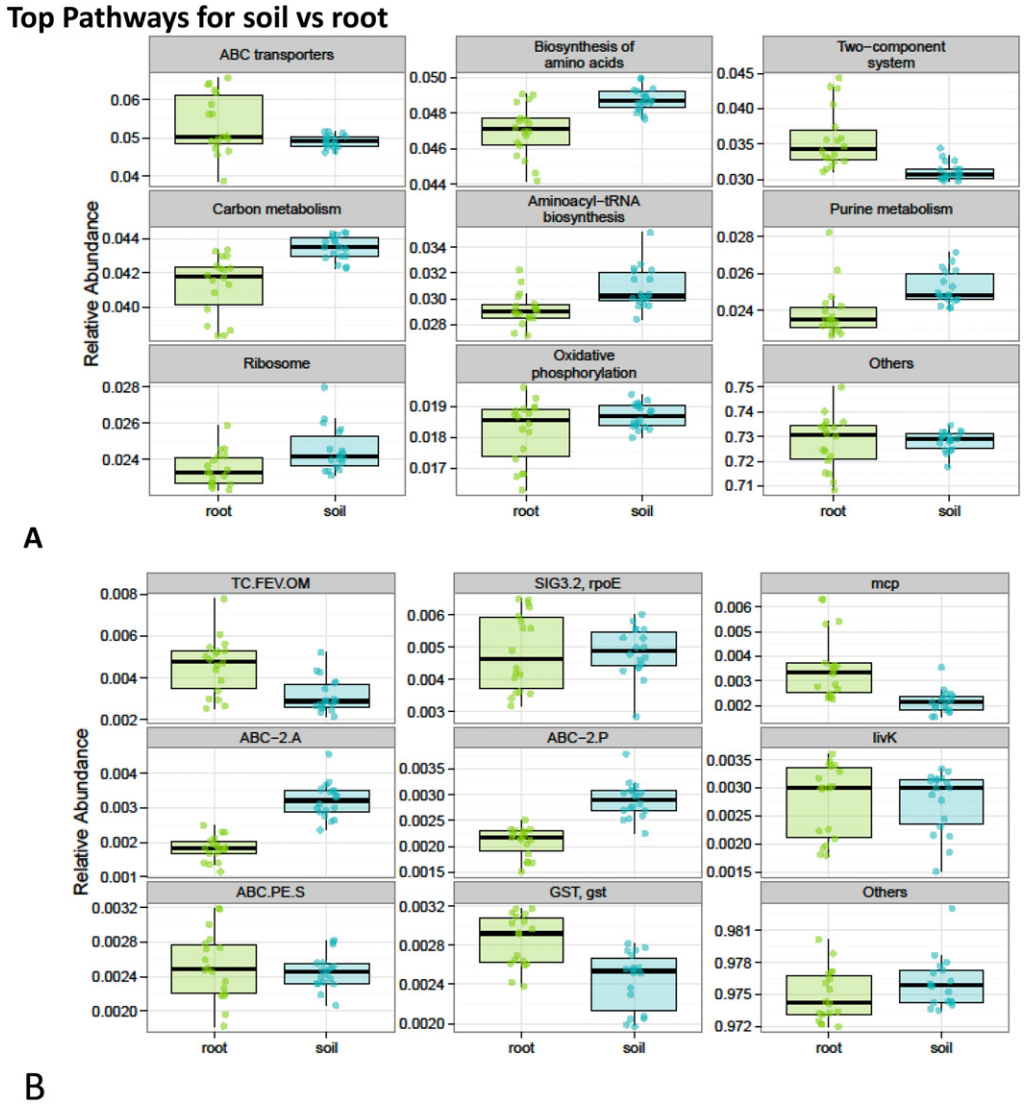

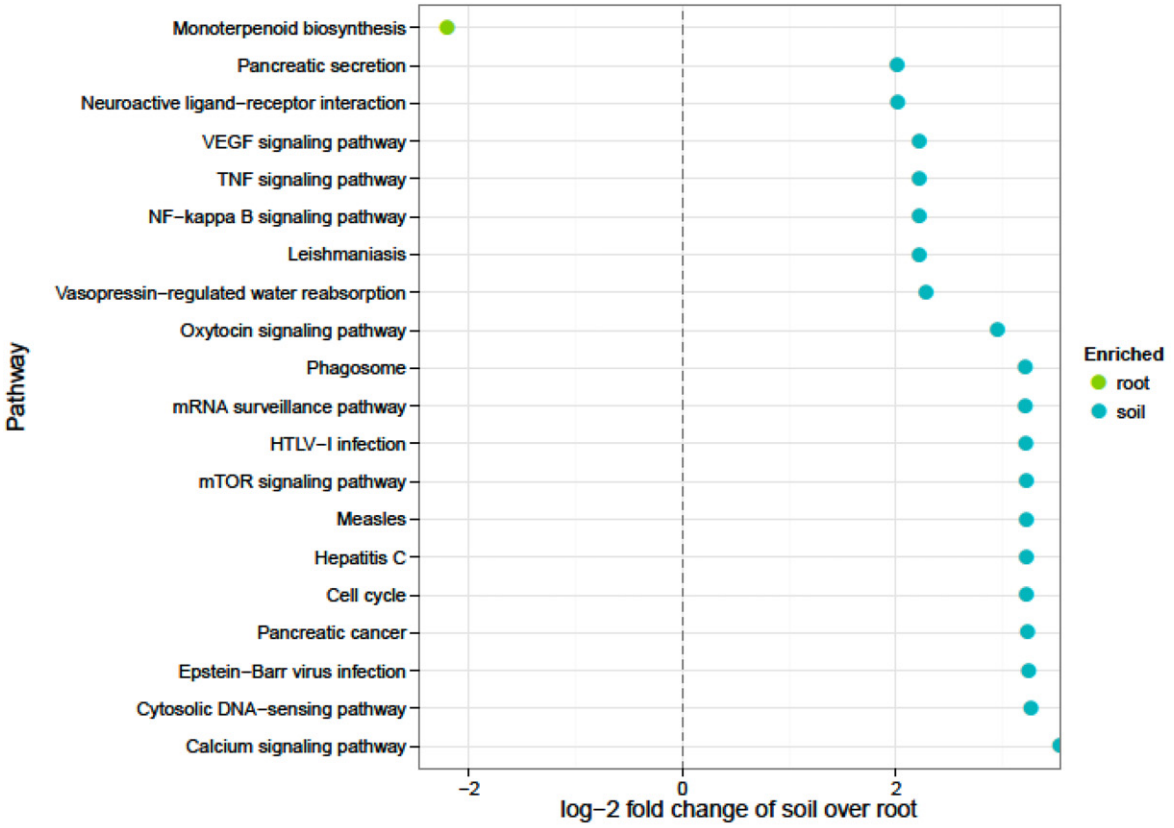
Monoterpenoid biosynthesis
Pancreatic secretion
Neuroactive ligand−receptor interaction
VEGF signaling pathway
TNF signaling pathway
NF−kappa B signaling pathway
Leishmaniasis
Vasopressin−regulated water reabsorption
Oxytocin signaling pathway
Phagosome
mRNA surveillance pathway
HTLV−I infection
mTOR signaling pathway
Measles
Hepatitis C
Cell cycle
Pancreatic cancer
Epstein−Barr virus infection
Cytosolic DNA−sensing pathway
Calcium signaling pathway
Pathway
−2
0
2
log−2 fold change of soil over root
Enriched
root
soil

C

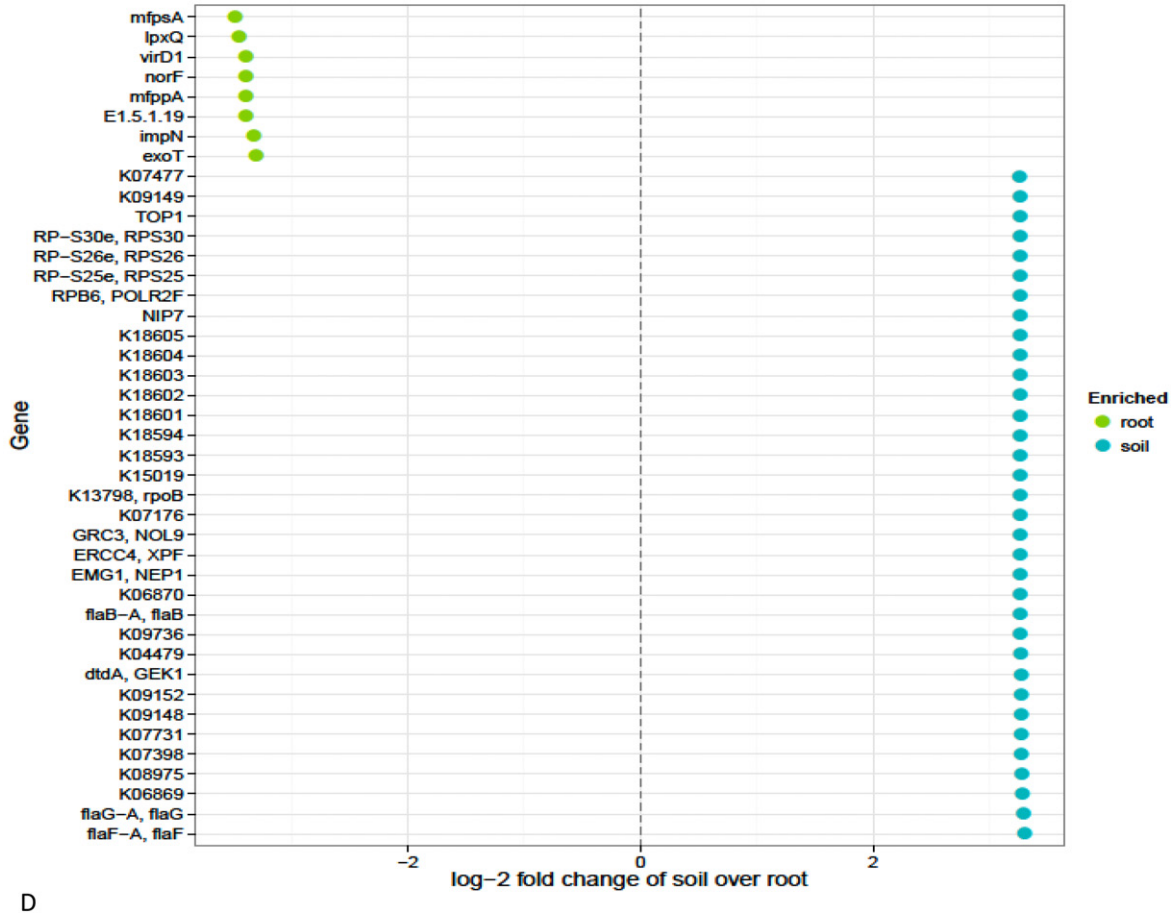
mfpsA
lpxQ
virD1
norF
mfppA
E1.5.1.19
impN
exoT
K07477
K09149
TOP1
RP−S30e, RPS30
RP−S26e, RPS26
RP−S25e, RPS25
RPB6, POLR2F
NIP7
K18605
K18604
K18603
K18602
K18601
K18594
K18593
K15019
K13798, rpoB
K07176
GRC3, NOL9
ERCC4, XPF
EMG1, NEP1
K06870
flaB−A, flaB
K09736
K04479
dtdA, GEK1
K09152
K09148
K07731
K07398
K08975
K06869
flaG−A, flaG
flaF−A, flaF
Gene
−2
0
2
log−2 fold change of soil over root
Enriched
root
soil

D

3. Results

3.1. Bacterial community composition between aboveground and belowground spinach microbiome

Overall, microbiome composition was significantly ($p = 0.001$) driven by sample type (soil, rhizosphere, and phyllosphere) and by season ($p = 0.003$), but not by salinity ($p = 0.568$) based on Bray-Curtis distance between microbiome samples using the PCoA ordination method. Compositional differences based on sample type and seasons were also reflected in the sample beta-diversity using weighted abundances (Fig. 1). Although March was cooler than both May and June, root and soil microbiome samples in March and May were more similar than those isolated in June, based on dimensional reduction of the Bray-Curtis distance between microbiome samples, using the PCoA ordination method (Fig. 1). Samples formed three clusters based on sample type and months when first separated along the primary axis (axis 1) according to sample type. Separation along axis 2 was based on months with root and soil samples from June separated from those collected in March and May. Overall, 56% of the sample variations were explained by the two major axes. Salinity significantly affected root microbiome beta-diversity using weighted abundances ($p = 0.032$) but did not significantly affect the relative abundances of microbial taxa ($p = 0.568$) based on PERMANOVA. This was confirmed by hierarchical clustering by the Ward method and Bray-Curtis distance (Fig. S1). According to our results, samples formed two primary clusters with leaf samples separated from root and soil samples; then sub-clustered by month. Samples did not cluster by any other covariate. Seasonal variations significantly ($p = 0.003$) affected the beta-diversity using weighted abundances for both soil and root sample types, but not leaf microbiome ($p = 0.057$). Soil samples had higher alpha diversity than root or leaf samples (Fig. 2). This was reflected by the higher Shannon diversity indices observed from soil samples. Looking at specific sample type, higher alpha diversity was observed in May than in June and March from leaf microbiome. This result was different from that obtained from soil and root samples, which showed no differences (Fig. 2).

Sequencing per sample ranged from a minimum of 68,440 to a maximum 717,922 filtered reads (Fig. 3). Rarefaction curves with an average number of OTUs detected versus sequencing library size show curves approaching a horizontal slope is nearly saturated, with few new OTUs undiscovered (Fig. S2). A curve with a steep slope remaining in the plot has not been sequenced to saturation, and substantial quantities of additional OTUs are expected upon further sequencing. Across the three sample types, *Proteobacteria*, *Cyanobacteria*, and *Bacteroidetes*-accounted for 77.1% of taxa detected in the rhizosphere, and *Proteobacteria*, *Bacteroidetes*, and *Actinobacteria* accounted for 55.1% of taxa detected in soil, while *Proteobacteria*, *Firmicutes*, *Bacteroidetes*, and *Actinobacteria* accounted for 55.35% of taxa detected in the phyllosphere (Fig. 4). From our analysis, *Proteobacteria* were the most abundant phyla represented across all sample. Root and soil samples contained high relative abundances of *Bacteriodetes* and *Actinobacteria*.

3.2. Pathways and functional gene analysis of soil compared to roots

Eight of the most proportional abundance pathways for soil and roots were ABC transporters, biosynthesis of amino acids, two-component system, carbon metabolism, aminoacyl-tRNA biosynthesis, purine metabolism, ribosome, and oxidative phosphorylation (Fig. 5). ABC transporters and two-component system pathways had higher relative percent mean in the root samples when compared to the soil samples. Biosynthesis of amino acids, carbon metabolism, aminoacyl-tRNA biosynthesis, and purine metabolism had higher mean relative percentages in soil as compared to root samples (Fig. 5A). The most abundant functional genes were related to transport systems and membrane receptor proteins (Fig. 5B). Percent relative mean values of two of the most abundant membrane receptor proteins were RNA polymerase sigma70 factor, ECF subfamily (SIG3.2, rpoE) and iron complex outer-membrane receptor protein (TC.FEV.OM). However, the relative proportions were not significantly different from each other as well as between rhizosphere and soil samples. Also, the percent relative abundances of the transport genes were not significantly different from each other, but the percent relative concentrations of ABC-2 type transport system ATP-binding protein (ABC-2. A) and ABC-2 type transport system permease protein (ABC-2.P) were significantly different between soil and rhizosphere samples (Fig. 5B). Furthermore, KEGG pathway prediction feature selection identified 126 pathways that were differentially abundant between the soil and root samples (Fig. 5C, Table S1). Only the 20 functional pathways with a log 2-fold change >2 are shown. The monoterpenoid biosynthesis pathway was one of the 97 pathways significantly enriched in rhizosphere samples. Signaling pathway for calcium was one of the 29 pathways enriched in soil samples (data not shown). There were 2198 significantly different genes detected between soil and root samples (Fig. 5D). About 871 genes were significantly enriched in soil samples and 1327 genes were significantly enriched in rhizosphere samples. Only the 42 genes with a log 2-fold change >3.3 are shown. Gene names are listed in Table S2. Functional gene and pathway profiles were inferred from the observed 16S rRNA OTUs using Piphillin (Iwai et al., 2016). Across all 54 samples, 7283 genes and 312 pathways were inferred from the 19,188 OTUs observed.

3.3. Pathways and functional genes analysis of rhizosphere (root) compare to leaf

The relative percent of the most abundant pathways between the rhizosphere and leaf surface microbiome were biosynthesis of amino acids, ABC transporters, ribosome, two-component systems, carbon metabolism, aminoacyl-tRNA biosynthesis, purine metabolism, and pyrimidine metabolism (Fig. 6A). Large variabilities (standard deviations) were observed in most of the leaf pathways as compared to root pathways and the large variations were associated with biosynthesis of amino acids, ABC transporters, ribosome, aminoacyl-tRNA biosynthesis, two-component system, purine metabolism, and pyrimidine metabolism (Fig. 6A). This is quite different from what was observed between soil and the rhizosphere, where higher variations in pathways were observed in the rhizosphere than in soil. At the gene level, the proportional abundance of the top eight inferred genes encoded for outer-membrane receptor proteins from the iron complex (TC.FEV.OM), methyl-accepting chemotaxis protein (MCP), RNA polymerase sigma70 factor, ECF subfamily (SIG3.2, rpoE), peptide/nickel transport system substrate-binding protein (ABC.PE.S), glutathione transferase (GST), iron complex outer- membrane receptor protein (TC.FEV.OM), tRNA Arg, tRNA Leu and tRNA Met (Fig. 6B). A summary of functional pathway prediction feature selection based on KEGG pathway prediction showed

Fig. 5. (A). Proportional abundance of the top inferred pathways for soil vs root. Plot shows the most abundant inferred pathways. Mean and standard deviation (sd) values are for percent relative abundances of the top 8 pathways. (B). Proportional abundance of the top inferred genes for soil vs root. Plot shows the most abundant functional genes. Mean and standard deviation (sd) are values for percent relative abundances of the top 8 genes. ABC-2.A; ABC-2 type transport system ATP-binding protein, ABC-2.P; ABC-2 type transport system permease protein, ABC.PE.S; peptide/nickel transport system substrate- binding protein, GST, gst; glutathione Strans-ferase, livK; branched-chain amino acid transport System sub-binding protein, mcp; methyl-accepting chemo- taxis protein, SIG3.2, rpoE; RNA polymerase sigma70 factor, ECF subfamily, TC.FEV.OM; iron complex outer- membrane receptor protein. (C). KEGG pathway prediction feature selection for soil vs root. Graphic summary of functional pathway prediction feature selection. (D). KEGG ortholog prediction feature selection for soil vs root. Graphic summary of functional gene prediction feature selection.

that 82 pathways were significantly different between the leaf and root samples (Fig. 6C), and 81 of the pathways were enriched in root samples. Only one pathway, phosphotransferase system, was enriched in leaf relative to root samples. At the gene level, 2523 genes were significantly enriched between the leaf and root samples (Fig. 6D) and 896 genes were enriched in leaf samples and 1627 genes were enriched in root samples.

4. Discussion

4.1. Soil, salinity, and drought interactions

This study aimed to characterize the agricultural microbiome shifts under drought/salinity conditions, performed under varying soil salinities in an outdoor lysimeter system cultivated with spinach. Spinach

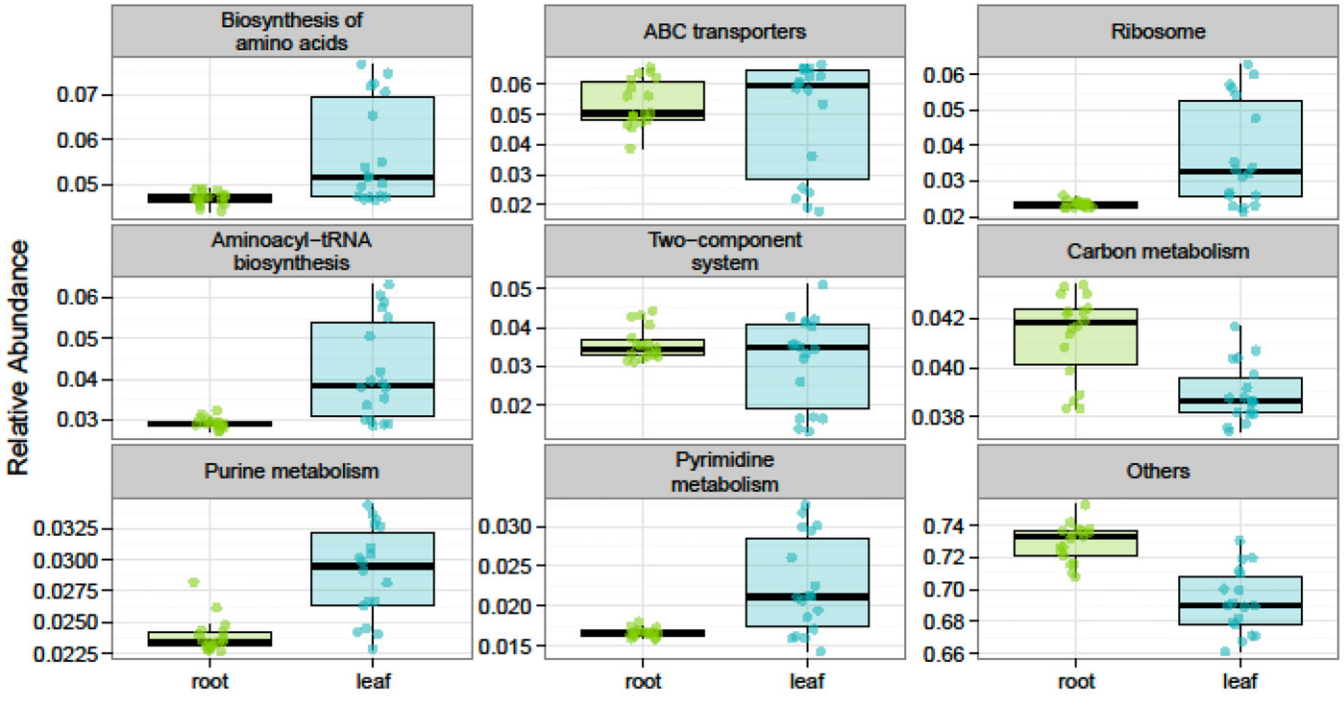

A

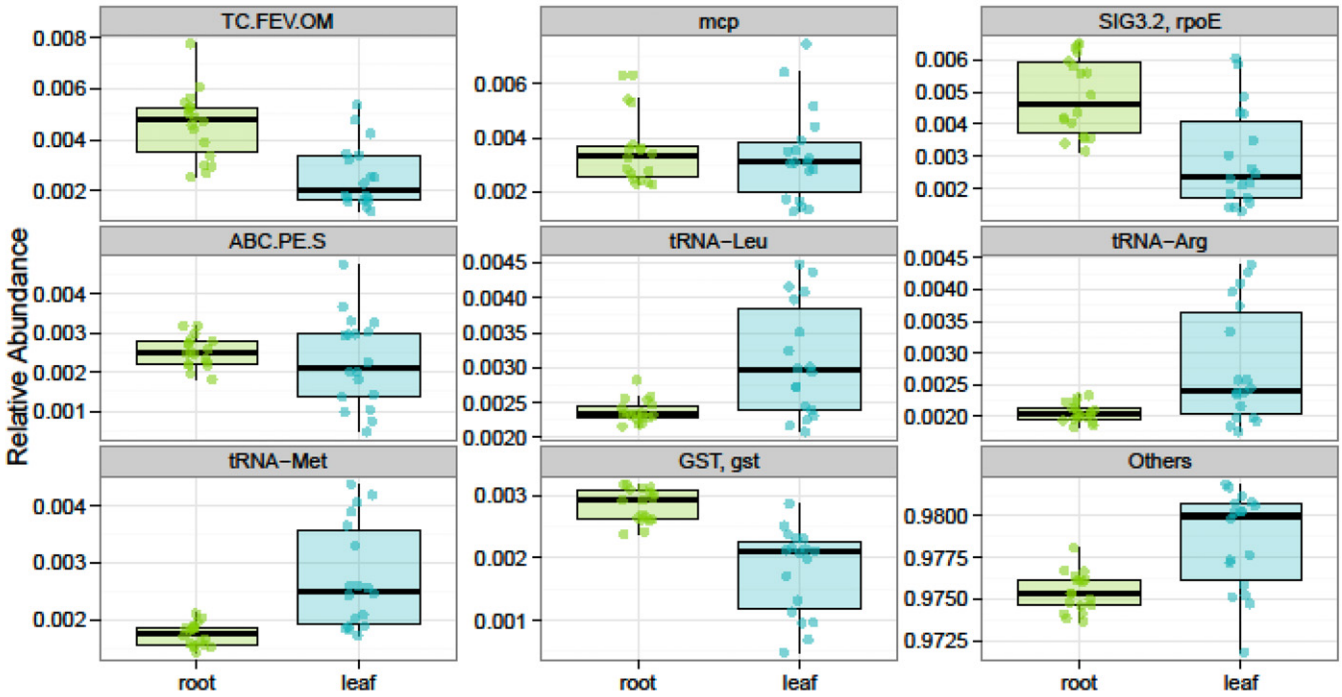

B

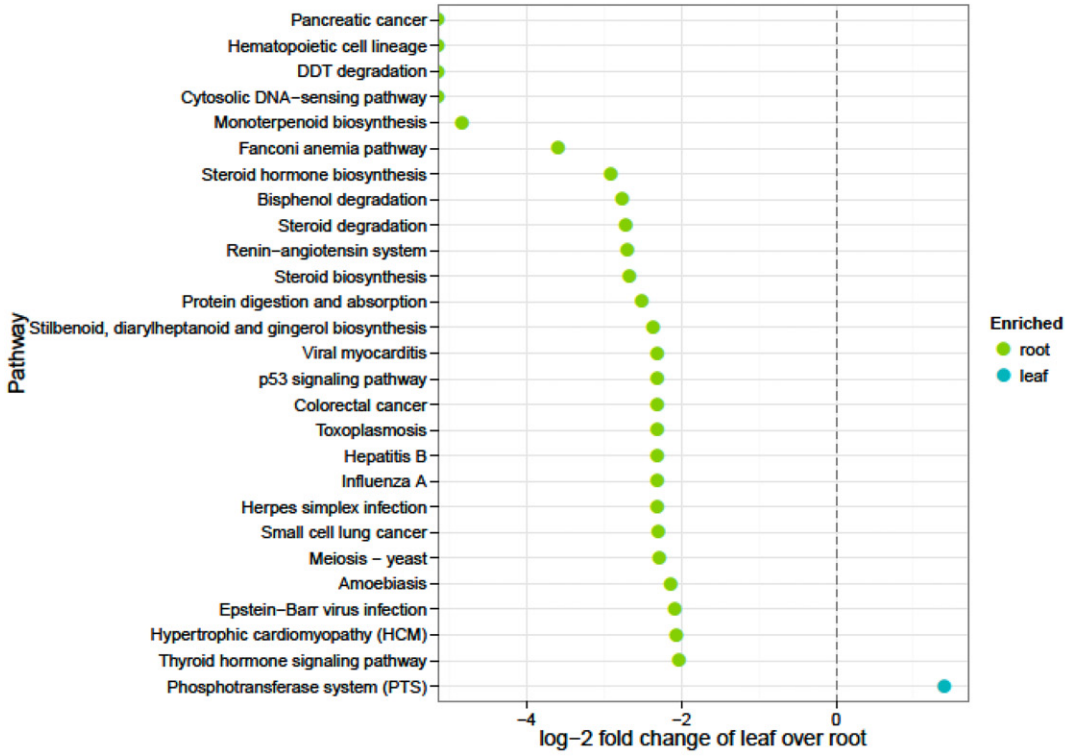
Pancreatic cancer
Hematopoietic cell lineage
DDT degradation
Cytosolic DNA−sensing pathway
Monoterpenoid biosynthesis
Fanconi anemia pathway
Steroid hormone biosynthesis
Bisphenol degradation
Steroid degradation
Renin−angiotensin system
Steroid biosynthesis
Protein digestion and absorption
Stilbenoid, diarylheptanoid and gingerol biosynthesis
Viral myocarditis
p53 signaling pathway
Colorectal cancer
Toxoplasmosis
Hepatitis B
Influenza A
Herpes simplex infection
Small cell lung cancer
Meiosis − yeast
Amoebiasis
Epstein−Barr virus infection
Hypertrophic cardiomyopathy (HCM)
Thyroid hormone signaling pathway
Phosphotransferase system (PTS)
Pathway
−4
−2
0
log−2 fold change of leaf over root
Enriched
root
leaf

C

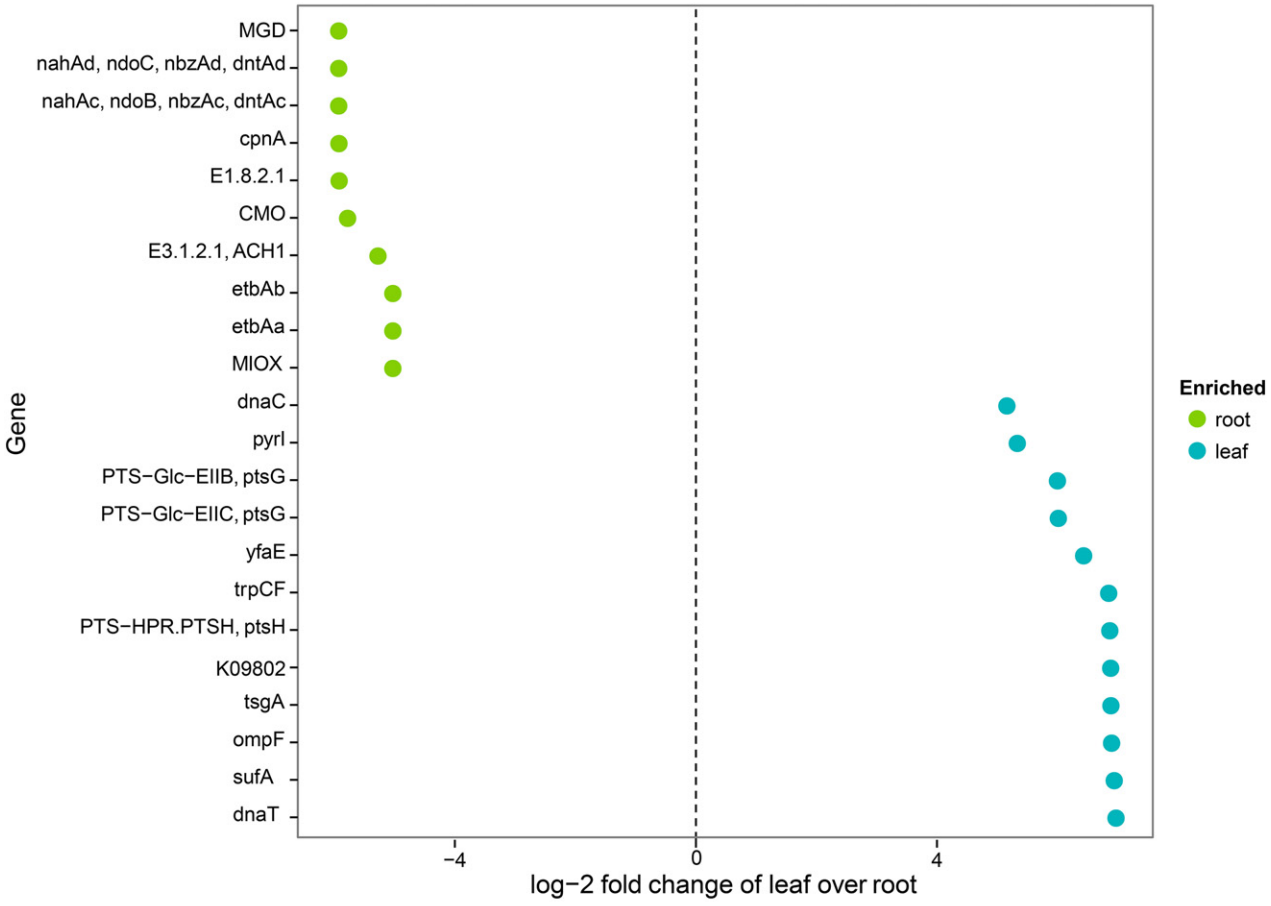
MGD
nahAd, ndoC, nbzAd, dntAd
nahAc, ndoB, nbzAc, dntAc
cpnA
E1.8.2.1
CMO
E3.1.2.1, ACH1
etbAb
etbAa
MIOX
dnaC
pyrI
PTS−Glc−EIIB, ptsG
PTS−Glc−EIIC, ptsG
yfaE
trpCF
PTS−HPR.PTSH, ptsH
K09802
tsgA
ompF
sufA
dnaT
Gene
−4
0
4
log−2 fold change of leaf over root
Enriched
root
leaf

D

optimal growth condition is between 15 and 20 °C (FES, 2005) and in this study, the average monthly temperatures during the growing periods of experiment I, II and III were 15.94 °C, 17.9 °C, 20.15 °C. During the planting seasons, water demands were different due to contrasting differences in evapotranspiration, driven by differences in temperature. These differences in temperatures resulted in significant ET_0 effects on soil microbial composition during the three planting seasons. It was also observed that $EC_{iw} = 9$ dS/m water did not cause any yield loss in the first experiment (March), therefore irrigation water treatments of EC_{iw} of 12 and 15 dS/m were added to experiments II and III (May and June). In these experiments, there was a relative shoot yield increase at low salinity levels and then a decrease in yield at the higher salinity levels (Ors and Suarez, 2016). In contrast to experiment I, experiments II and III had yield losses at $EC_{iw} = 9$ dS/m. However fresh weights of plants were higher at EC 4 and 7 dS/m treatments compared to the controls in experiments II and III, as were observed for experiment I (Ors and Suarez, 2016). The growing period was the longest for the first experiment, due to temperatures below the optimum for the crop, shorter for the second experiment, and the shortest for the third experiment. This is consistent with the fact that temperatures increased drastically from one growth period to the next in experiments I-III. Ors and Suarez (2016) recently reported that during the first experiment, ET_0 was very low during the first ten days, averaging 1.96 mm d^{-1}. However, ET_0 values were 4.43- and 6.36-mm $d^{-1}$for experiments II and III, respectively. The high temperature corresponded with increasing solar radiation from the experiment I to III, although relative humidity was similar for the three experiments based on CIMIS weather station no. 44 at the University of California Riverside (Ibekwe et al., 2017).

4.2. Microbial community composition

Results suggest that drought was a significant factor driving changes in microbial composition. A key question regarding the distinct bacterial communities in lysimeter soils concerns the environmental parameters responsible for these differences, especially given that salinity did not significantly affect the relative abundances of microbial taxa. For DNA phylotypes, seasonal variation (temperature) was the only significant predictor of alpha diversity, with the most significant differences observed on leaf surfaces (Fig. 2) and leaf surface temperature affecting leaf microbiome moderately. These data support the hypothesis that seasonal variations are important ecological factors affecting microbial dynamics. This observation may be different with different plants or genotypes, because it has been observed that microbial community composition varies by plant genotype, suggesting that plant genotype can select for soil microbial characteristics (Aira et al., 2010). However, in another study, it was observed that rather than community divergence between cultivars, the divergence between soils substantially contributed to microbiome variation (Chen et al., 2017).

Our study also showed that salinity had a significant effect on microbial diversity. This implies that once diversity is established and the composition of the community is set, the community members are therefore adapted to the salinity stress, and the dominant members of the community continue to sustain themselves due to environmental adaptation (Fig. SI). Our study also showed that salinity effect on soil microbial diversity was also dependent on the salinity range they experienced. This is consistent with our previous study in the same lysimeter plots using cucumber as test plants that showed that soil and rhizosphere developed its own microbial communities in correlation with distinctly different salinity regimes (Ibekwe et al., 2010). It is a known factor that high salinity in combination with severe water stress may be one of the most stressful combinations affecting soil microbial diversity (de Souza Silva and Fay, 2012). This phenomenon has been previously explained (Oren, 2002a, 2002b; Oren, 2013) in a way that life in high salt concentrations is bioenergetically taxing, and microorganisms must maintain osmotic equilibrium between the cytoplasm and the surrounding medium for the exclusion of sodium ions from inside the cell.

4.3. Changes in metabolic pathways and functional genes based on Piphillin

Changes in metabolic pathways and functional genes in this study were based on Piphillin algorithm predictions (Iwai et al., 2016) to generate inferred metagenomes of sample type microbial communities based on a 97% identity cutoff. About 25.8% of the sample type microbial communities were assigned to genomes by the Piphillin algorithm at the 97% level with a Mantel correlation (Mantel's $r = 0.58$; $P < 0.001$) between the distance matrices and predicted metagenomic compositions of the sample types. This observation was low but other studies have captured the same low correlation between the distance metrics based on phylogenetic/taxonomic and predicted the metagenomic composition of their samples (Poret-Peterson et al., 2019; Noah et al., 2019).

From a large amount of data available on transcript-profiling studies in plants subjected to drought and salt (Chaves et al., 2009), it is becoming apparent that plants perceive and respond to these stresses by quickly altering gene expression in parallel with physiological and biochemical alterations under mild to moderate stress conditions. These authors noted that in comparison with drought, salt stress affected more genes and more intensely, possibly reflecting the combined effects of dehydration and osmotic stress in salt-stressed plants (Chaves et al., 2009). We generated predicted metagenomes of drought and salinity communities to explore potential metabolic pathways of responsive taxa, especially in relation to other studies that have started to elucidate the mechanisms by which salinity and drought suppress targeted bacteria and plants. Monoterpenoid biosynthesis was the most significantly enriched pathway in root samples when compared to the soil samples (Fig. 5C). Monoterpenoids are a class of common secondary plant metabolites, and their production has been shown to be affected by water stress (Delfine et al., 2005). However, their synthesis is not exclusively limited to plants and genomic evidence suggests that monoterpene synthases are common to bacteria (Yamada et al., 2015).

The calcium signaling pathway was the most enriched pathway in soil samples when compared to root samples (Fig. 5D). Calcium has been shown to be affected by signals triggered by damage responses from microbes (Ranf et al., 2014) and is also an important molecular messenger for nitrate pathways in plants (Riveras et al., 2015). These metabolites have been confirmed in *Streptomyces* and *Kitasatospora* species. OTU picking resulted in about 14,000 OTUs which were classified into various predictive functional categories. The most abundant of these predicted functions were mapped to membrane transport, DNA repair and recombination, signal transduction, purine metabolism, translation-related protein processing, oxidative phosphorylation and bacterial motility protein secretion (Figs. 5B; 6B; Tables S1 and 2). Most of these functions are related to maintenance of cell function and structure which would be performed by every species in the community. The predictive abundances indicate that, functionally, root bacteria had the highest gene abundances (Figs. 5B and 6B). From our previous study (Ibekwe et al., 2017), sequencing data identified some microorganisms with relatively restricted salt concentration range for growth,

Fig. 6. (A). Proportional abundance of the top inferred pathways for root vs leaf. Plot shows the most abundant inferred pathways. Mean and standard deviation (sd) values are for percent relative abundances of the top 8 pathways. (B). Proportional abundance of the top inferred genes for root vs leaf. Plot shows the most abundant functional genes. Mean and standard deviation (sd) values are for percent relative abundances of the top 8 genes. (C). KEGG pathway prediction feature selection for root vs leaf. (D). KEGG gene ortholog prediction feature selection for root vs leaf. Graphic summary of functional pathway prediction feature selection.

as well as others such as *Halomonas elongata*, which is a well-known example of a bacterium that can adapt to life over the whole salt concentration range from fresh water of low salinity to halite saturation (Vreeland et al., 1980). During that study, the genus *Halomonas* were found in the soil and in the rhizosphere samples with different salinity concentrations. Their relative percent concentrations were significantly higher ($P = 0.036$) in June than in May in the rhizosphere, indicating that increasing salinity stress to the levels tested in this study did not affect them. The important osmoregulatory mechanism that allows *Halomonas elongata* to cope with high salinities is the ability to amass water-soluble organic compounds, which do not disturb the cell's metabolism even at high cytoplasmic concentrations (Kindzierski et al., 2017). Ectoine is synthesized in the cell cytoplasm as one of the main compatible solute (Ono et al., 1999; Galinski and Oren, 1991; Wohlfarth et al., 1990). Bacteria have specific genes, which encode proteins that function in glucose degradation, anaplerosis and the TCA cycle, nitrogen metabolism, ectoine synthesis, ectoine degradation, and in ectoine transport (Kindzierski et al., 2017).

Our data suggest that salinity and drought affected the above- and belowground spinach microbiomes differently, with salinity negatively impacting soil and root microbiomes and causing taxonomic and functional differences between the two sample types, but not with leaf microbiome. Assemblages from leaves based on alpha diversity were significantly higher in May than in June and March, but no significant effect was observed in soil and roots because of season or temperature. In terms of potential function, the use of piphillin allowed the identification of diverse genes conferring salt resistance to the above- and belowground microbiome encoding for well-known proteins involved in osmoadaptation between soil and roots, such as transport-binding proteins, transport system permease proteins, glycerol permease and proton pump, proteins related to repair, replication and transcription of nucleic acids, transport system substrate-binding protein, chemo-taxis protein, RNA and DNA helicases and even an endonuclease III. Our data agrees with the expected assemblage of organisms thriving in an environment affected by moderate to severe salinity.

Declaration of competing interest

The authors declare no conflict of interest.

Acknowledgements

This research was supported by the 212 Manure and Byproduct Utilization Project of the USDA ARS Project # 036012036505. We thank Ronak Patel for technical assistance. Mention of trade names or commercial products in this publication is solely for the purpose of providing specific information and does not imply recommendation or endorsement by the U.S. Department of Agriculture. The U.S. Department of Agriculture (USDA) prohibits discrimination in all its programs and activities on the basis of race, color, national origin, age, disability, and where applicable, sex, marital status, familial status, parental status, religion, sexual orientation, genetic information, political beliefs, reprisal, or because all or part of an individual's income is derived from any public assistance program.

Appendix A. Supplementary data

Supplementary data to this article can be found online at https://doi.org/10.1016/j.scitotenv.2020.137207.

References

Aira, M., Gomez-Brandon, M., Lazcano, C., Bååth, E., Dominguez, J., 2010. Plant genotype strongly modifies the structure and growth of maize rhizosphere microbial communities. Soil Biol. Biochem. 42, 2276–2281.

Aßhauer, K.P., Wemheuer, B., Daniel, R., Meinicke, P., 2015. Tax4Fun: predicting functional profiles from metagenomic 16S rRNA data. Bioinformatics 31, 2882–2884.

Bardgett, R.D., 2018. Linking aboveground–belowground ecology: a short historical perspective. In: Ohgushi, T., Wurst, S., Johnson, S. (Eds.), Aboveground–Belowground Community Ecology. Ecological Studies (Analysis and Synthesis). 234. Springer, Cham.

Benjamini, Y., Hochberg, Y., 1995. Controlling the false discovery rate: a practical and powerful approach to multiple testing. J. R. Stat. Soc. Ser. B (Stat Methodol.) 57, 289–300.

Bringel, F., Couée, I., 2015. Pivotal roles of phyllosphere microorganisms at the interface between plant functioning and atmospheric trace gas dynamics. Frontier in Microbiol 6, 486. https://doi.org/10.3389/fmicb.2015.00486.

Caporaso, J.G., Lauber, C., Walters, W.A., Berg-Lyons, D., Lozupone, C.A., Turnbaugh, P.J., et al., 2011. Global patterns of 16S rRNA diversity at a depth of millions of sequences per sample. PNAS 15, 4516–4522.

Chaves, M.M., Flexas, J., Pinheiro, C., 2009. Photosynthesis under drought and salt stress: regulation mechanisms from whole plant to cell. Annals of Bot 103, 551–560.

Chen, L., Xin, X., Zhang, J., Redmile-Gordon, M., Nie, G., 2017. Soil characteristics overwhelm cultivar effects on the structure and assembly of root-associated microbiomes of modern maize. Pedosphere 17, 60370–60379.

Chhabra, R., 1996. Soil Salinity and Water Quality. Balkema, Rotterdam, The Netherlands.

de Souza Silva, C.M.M., Fay, E.F., 2012. In: Hernandez Soriano, M.C. (Ed.), Effect of Salinity on Soil Microorganisms, Soil Health and Land Use Management http://www.intechopen.com/books/soil-health-and-land-usemanagement/effect-of-salinity-onsoil-microorganisms (ISBN: 978-953-307-614-0, InTech, Available from:).

Delfine, S., Loreto, F., Pinelli, P., Tognetti, R., Alvino, A., 2005. Isoprenoids content and photosynthetic limitations in rosemary and spearmint plants under water stress. Agric. Ecosyst. Environ. 106, 243–252.

Edgar, R.C., 2010. Search and clustering orders of magnitude faster than BLAST. Bioinformatics 26, 2460–2461.

Edgar, R.C., 2013. UPARSE: highly accurate OTU sequences from microbial amplicon reads. Nat. Methods 10, 996–998.

FES, 2005. Spinach: Atlantic Provinces Vegetable Crops Production Guide, No. 1400A. Department of Agriculture, Fisheries and Aquaculture. Farm Extension Services, Canada.

Froelich, B.A., Williams, T.C., Noble, R.T., Oliver, J.D., 2012. Apparent loss of Vibrio vulnificus from North Carolina oysters coincides with a drought-induced increase in salinity. Appl. Environ. Microbiol. 78, 3885–3889.

Furnkranz, M., Wanek, W., Richter, A., Abell, G., Rasche, F., Sessitsch, A., 2008. Nitrogen fixation by phyllosphere bacteria associated with higher plants and their colonizing epiphytes of a tropical lowland rainforest of Costa Rica. ISME J 2, 561–570.

Galinski, E.A., Oren, A., 1991. Isolation and structure determination of a novel compatible solute from the moderately halophilic purple sulfur bacterium *Ectothiorhodospira marismortui*. European J. Biochem. 198, 593–598.

Hellberg, R.S., Chu, E., 2015. Effects of climate change on the persistence and dispersal of foodborne bacterial pathogens in the outdoor environment: a review. Crit. Rev. Microbiol. https://doi.org/10.3109/1040841X.2014.972335.

Ibekwe, A.M., Poss, J.A., Grattan, S.R., Grieve, C.M., Suarez, D., 2010. Bacterial diversity in cucumber (*Cucumis sativus*) rhizosphere in response to salinity, soil pH, and boron. Soil Biol. Biochem. 42, 567–575.

Ibekwe, A.M., Ors, S., Ferreira, J.F.S., Liu, X., Suarez, D.L., 2017. Seasonal induced changes in spinach rhizosphere microbial community structure with varying salinity and drought. Sc. Total Environ. 579, 1485–1495.

Iwai, S., Weinmaier, T., Schmidt, B.L., Albertson, D.G., Poloso, N.J., Dabbagh, K., DeSantis, T.Z., 2016. Piphillin: improved prediction of metagenomic content by direct inference from human microbiomes. PLoS One 11 (11), e0166104.

Jansson, J.K., Hofmockel, K.S., 2018. The soil microbiome — from metagenomics to metaphenomics. Current Opinion Microbiol 43, 162–168 2018.

Karl, T.R., Melillo, J.M., Peterson, T.C., 2009. Global Climate Change Impacts in the United States. Cambridge University Press, New York.

Kindzierski, V., Raschke, S., Knabe, N., Siedler, F., Scheffer, B., Pflüger-Grau, K., et al., 2017. Osmoregulation in the Halophilic bacterium *Halomonas elongata*: a case study for integrative systems biology. PLoS One 12 (1), e0168818. https://doi.org/10.1371/journal.pone.0168818.

Klute, A., 1986. Water retention: laboratory methods. In: Klute, A. (Ed.), Methods of Soil Analysis, Part 1, Physical and Mineralogical Methods. Soil S. Soc. America Inc, Madison, Wisconsin.

Koike, S.T., Cahn, M., Cantwell, M., Fennimore, S., Lestrange, M., Natwick, E., Smith, R.F., Takele, E., 2011. In: University of California. Agric. Natural Res. Pub (Ed.), Spinach Production in California, p. 7212.

Koo, H., Hakim, J.A., Morrow, C.D., Eipers, P.G., Davila, A., Andersen, D.T., Bej, A.K., 2017. Comparison of two bioinformatics tools used to characterize the microbial diversity and predictive functional attributes of microbial mats from Lake Obersee. Ant. J. Microbiolog. Methods. 140, 15–22.

Langille, M.G., Zaneveld, J., Caporaso, J.G., McDonald, D., Knights, D., Reyes, J.A., Clemente, J.C., Burkepile, D.E., Thurber, R.L.V., Knight, R., Beiko, R.G., 2013. Predictive functional profiling of microbial communities using 16S rRNA marker gene sequences. Nat. Biotech. 31, 814–821.

Love, M.I., Huber, W., Anders, S., 2014. Moderated estimation of fold change and dispersion for RNA-Seq data with DESeq2. bioRxiv https://doi.org/10.1101/002832.

McDonald, D., Price, M.N., Goodrich, J., Nawrocki, E.P., DeSantis, T.Z., Probst, A., Andersen, G.L., Knight, R., Hugenholtz, P., 2012. An improved Greengenes taxonomy with explicit ranks for ecological and evolutionary analyses of bacteria and archaea. ISME J 6, 610–618.

McMurdie, P.J., Holmes, S., 2013. phyloseq: an R package for reproducible interactive analysis and graphics of microbiome census data. PLoS One 8, e61217.

Newton, A.C., Gravouil, C., Fountaine, J.M., 2010. Managing the ecology of foliar pathogens: ecological tolerance in crops. Ann. Appl. Biol. 157, 343–359.

Noah, W., Soko, N.W., Bradford, M.A., 2019. Microbial formation of stable soil carbon is more efficient from belowground than aboveground input. Nat. Geosci. 12, 46–53.

Ono, H., Sawada, K., Khunajakr, N., Tao, T., Yamamoto, M., Hiramoto, M., et al., 1999. Characterization of biosynthetic enzymes for ectoine as a compatible solute in a moderately halophilic eubacterium, *Halomonas elongata*. J. Bacteriol. 181, 91–99.
Oren, A., 1999. Bioenergetic aspects of halophilism. Microbiol. Mol. Biol. Rev. 63, 334–340.
Oren, A., 2002a. Molecular ecology of extremely halophilic archaea and bacteria. FEMS Microbiol. Ecol. 39, 1–7.
Oren, A., 2002b. Diversity of halophilic microorganisms: environments, phylogeny, physiology, and applications. J. Indust. Microbiol. Biotech. 28, 56–63.
Oren, A., 2013. Life at high salt concentrations. In: Rosenberg, et al. (Eds.), The Procharyotes- Prokaryotes Communities ans Ecophysiology. https://doi.org/10.1007/978-3-642-30123-0_57 (Berlin Heidelberg).
Ors, S., Suarez, D.L., 2016. Salt tolerant of spinach as related to seasonal climate. Hort. Scince (Prague). 43, 33–41.
Ors, S., Suarez, D.L., 2017. Spinach biomass yield and physiological response to interactive salinity and water stress. Agric. Water Manag. 190, 31–41.
Poret-Peterson, A.T., Albu, S., McClean, A.E., Kluepfel, D.A., 2019. Shifts in soil bacterial communities as a function of carbon source used during anaerobic soil disinfestation. Front. Environ. Sc. 6, 160. https://doi.org/10.3389/fenvs.2018.00160.
Poss, J., Russell, W., Shouse, P., Austin, R., Grattan, S., Grieve, C., Lieth, J., Zeng, L., 2004. A volumetric lysimeter system (VLS): an alternative to weighing lysimeters for plant-water relations studies. Comp. Electronics Agric. 43, 55–68.
Ranf, S., Eschen-Lippold, L., Fröhlich, K., Westphal, L., Scheel, D., Lee, J., 2014. Microbe- associated molecular pattern-induced calcium signaling requires the receptor-like cytoplasmic kinases, PBL1 and BIK1. BMC Plant Biol. 14 379–15.
Riveras, E., Alvarez, J.M., Vidal, E.A., Oses, C., Vega, A., Gutiérrez, R.A., 2015. The calcium ion is a second messenger in the nitrate signaling pathway of arabidopsis. Plant Physiol. 169, 1397–1404.
Sokol, N.W., Bradford, M.A., 2018. Microbial formation of stable soil carbon is more efficient from belowground than aboveground input. Nat. Geosci. 12, 46–53. https://doi.org/10.1038/s41561-018-0258-6.
Suarez, D.L., Taber, P., 2012. Extractchem. Available at. https://www.ars.usda.gov/research/software/?modeCode=20-36-05-00.
USEPA, 2004. Guidelines for Water Reuse. EPA 625/R-04/108. USEPA, Cincinnati, OH.
Vreeland, R.H., Litchfield, C.D., Martin, E.L., Elliot, E., 1980. *Halomonas elongata*, a new genus and species of extremely salt-tolerant bacteria. International J. Syst. Bacteriol. 30, 485–495.
Wohlfarth, A., Severin, J., Galinski, E.A., 1990. The spectrum of compatible solutes in heterotrophic halophilic eubacteria of the family Halomonadaceae. J. General Microbiol. 136, 705–712.
Yamada, Y., Kuzuyama, T., Komatsu, M., Shin-ya, K., Omura, S., Cane, D.E., et al., 2015. Terpene synthases are widely distributed in bacteria. PNAS 112, 857–862.